influence of wall radiation in 2D cavities heated from below

Eric Albin, Ronnie Knikker, Shihe Xin

▶ **To cite this version:**

Eric Albin, Ronnie Knikker, Shihe Xin. influence of wall radiation in 2D cavities heated from below. 16th International Heat Transfer Conference, IHTC-16, Aug 2018, Beijing, China. hal-01849866

HAL Id: hal-01849866
https://hal.science/hal-01849866v1

Submitted on 22 Oct 2018

HAL is a multi-disciplinary open access archive for the deposit and dissemination of scientific research documents, whether they are published or not. The documents may come from teaching and research institutions in France or abroad, or from public or private research centers.

L'archive ouverte pluridisciplinaire **HAL**, est destinée au dépôt et à la diffusion de documents scientifiques de niveau recherche, publiés ou non, émanant des établissements d'enseignement et de recherche français ou étrangers, des laboratoires publics ou privés.

INFLUENCE OF WALL RADIATION IN 2D CAVITIES HEATED FROM BELOW

Eric Albin, Ronnie Knikker, Shihe Xin[1]

Univ Lyon, CNRS, INSA-Lyon, Université Claude Bernard Lyon 1,
CETHIL UMR5008, F-69621, Villeurbanne, France

Abstract

This study investigates numerically the effects of wall radiation on Bénard cells in cavities heated from below using Chebyshev spectral methods. Bifurcation theory is also used to describe and analyse the cellular flow solutions obtained in a square and a rectangle cavities filled with air.

As wall radiation modifies the flow via the adiabatic vertical wall condition, the motionless and thermally stratified solution no longer exists at low Rayleigh numbers and is replaced by a very weak 2×2 cellular solution. This 4-cell weak flow undergoes pitchfork bifurcations at higher Rayleigh numbers: both perfect and imperfect pitchfork bifurcations are observed in the presence of wall radiation. Bifurcations to cellular flows with a reflection symmetry become imperfect because the cellular flows with the opposite rotating directions are no more equivalent. Therefore the resulting convective and radiative Nusselt numbers of the two bifurcated branches are no longer the same on the top or bottom wall. Note also that Nusselt numbers (either convective or radiative) of any bifurcated branch at one Rayleigh number are different on the bottom and top walls with wall radiation. Results obtained are analysed and some recommendations are given to describe Bénard flows with wall radiation.

Keywords: Rayleigh-Bénard, wall radiation, convection, bifurcation

1 Introduction

Heat transfer in a cavity heated from below has been widely investigated [1]. Nevertheless, few studies with wall radiation have been conducted and the effect of wall radiation is less understood in the litterature. Mizushima *et al.* [4] used bifurcation diagrams to describe various thermal and flow regimes in such a cavity without radiation. Such bifurcation analyses are not used in the past studies with radiative walls.

In [5], Ridouane *et al.* describe various steady-state patterns and unsteady solutions in a square cavity with radiative walls. They describe different flow solutions and heat regimes in various nested tables. For instance, they analyse bi-cellular flow regimes ascending at the middle of the cavity, but do not study the reverse solution descending at the middle. Also, the given convective and radiative Nusselt numbers are not associated to the top or bottom walls. The effect of vertical wall emissivity ($0 \leqslant \epsilon_V \leqslant 0.85$) and of cavity aspect-ratio ($1 \leqslant AR \leqslant 10$) on Rayleigh-Bénard convection is investigated in Gad and Balaji [1]. The numerical solutions are computed using FLUENT to solve steady incompressible Navier-Stokes equations with radiative walls and a transparent medium. They observe jumps from unicellular to bi-cellular flows at some critical Rayleigh numbers, but they do not address the problem of multiple solutions nor the issue of flow bifurcations. Some preliminary studies are presented by Xin *e*t al. [6, 7, 3]: the coupling of natural convection with surface radiation in a cavity using a Chebyshev spectral method is presented and validated and the first bifurcation at low Rayleigh number is studied for a square cavity and a twice longer cavity in [3].

The present study continues the work performed in [3], adopts bifurcation analyses used in [4] and suggests, for wall radiation cases, that results of Nusselt numbers should be presented for

[1]shihe.xin@insa-lyon.fr

both the top and bottom walls or at least for the specified wall (either top or bottom wall).

The paper is organized as follows. After recalling the governing equations of the cavity problem with wall radiation, the bifurcation theory is first used to describe the different flow regimes. Heat transfers at walls are therefore analyzed using Nusselt numbers. Some concluding remarks and recommendations end the paper.

2 Governing equations

A cavity of length L and height H is heated from below with a constant high temperature T_h at the bottom wall and cooled from top with a constant low temperature T_c at the top wall (see Fig. 1). Two aspect ratios are considered in this paper: a square cavity ($L = H$) and a rectangular cavity ($L = 2H$).

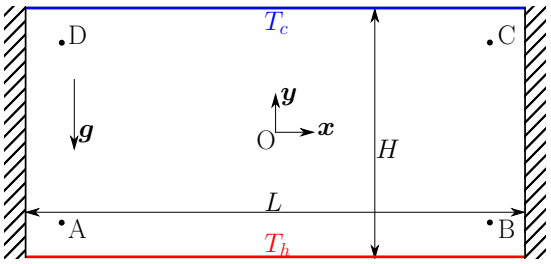

Figure 1: Geometry of the simulated cavity. Horizontal walls are isothermal and vertical walls are adiabatic. Points A, B, C and D are located at $\pm 0.1H$ from the corners.

The cavity is filled with air considered as a Newtonian transparent medium of density ρ, kinematic viscosity ν, thermal conductivity k, specific heat c_p, thermal diffusivity $\alpha = k/(\rho c_p)$ and thermal dilatation coefficient β. In order to make comparisons with the results of Gad and Balaji [1], the considered fluid properties are $T_0 = \frac{T_c+T_h}{2} = 309$ K, $\frac{g\cdot\beta}{\nu\cdot\alpha} = 8.0736 \cdot 10^7$ and $\mathrm{Pr} = \frac{\nu}{\alpha} = 0.71$ with $g = 9.81m \cdot s^{-2}$. Natural convection flow in such a cavity is governed by the Navier-Stokes equations and depends strongly on the Rayleigh number $\mathrm{Ra} = \frac{g\beta\Delta T H^3}{\nu\alpha}$ where $\Delta T = T_h - T_c$ is the differential temperature in the cavity. In presence of wall radiation, it also depends on a radiation to conduction parameter $\mathrm{Nr} = \sigma(T_h^4 - T_c^4) \cdot H/(k\Delta T)$ with $\sigma = 5.67 \cdot 10^{-8} W \cdot m^{-2} \cdot K^{-4}$ being the Stefan-Boltzmann constant. The Rayleigh number is changed by varying ΔT with $\mathrm{Nr} \simeq 4\sigma T_0^3 H/k = 7.765$ (i.e. $H = 3.14$cm to match [1] with $T_c = T_0 - \Delta T/2$ and $T_h = T_0 + \Delta T/2$). In this study, Navier-Stokes equations of the incompressible flow under the Boussinesq approximation are solved :

$$\frac{\partial u}{\partial x} + \frac{\partial v}{\partial y} = 0 \tag{1a}$$

$$\frac{\partial u}{\partial t} + u\frac{\partial u}{\partial x} + v\frac{\partial u}{\partial y} = -\frac{1}{\rho_0}\frac{\partial P}{\partial x} + \nu\left(\frac{\partial^2 u}{\partial x^2} + \frac{\partial^2 u}{\partial y^2}\right) \tag{1b}$$

$$\frac{\partial v}{\partial t} + u\frac{\partial v}{\partial x} + v\frac{\partial v}{\partial y} = g\beta(T - T_0) - \frac{1}{\rho_0}\frac{\partial P}{\partial y} + \nu\left(\frac{\partial^2 v}{\partial x^2} + \frac{\partial^2 v}{\partial y^2}\right) \tag{1c}$$

$$\rho_0 c_p\left(\frac{\partial T}{\partial t} + u\frac{\partial T}{\partial x} + v\frac{\partial T}{\partial y}\right) = k\left(\frac{\partial^2 T}{\partial x^2} + \frac{\partial^2 T}{\partial y^2}\right) \tag{1d}$$

A no-slip wall condition is forced at the walls ($u = v = 0$). The bottom and top walls of the cavity are isothermal walls ($T(y = -H/2) = T_h$ and $T(y = H/2) = T_c$). The two vertical walls are adiabatic in the sense that radiative transfer balances local heat conduction:

$$\underbrace{-k\frac{\partial T}{\partial x}}_{q_c} + q_r = 0 \quad \text{on left wall} \qquad \text{and} \qquad \underbrace{-k\frac{\partial T}{\partial x}}_{q_c} - q_r = 0 \quad \text{on right wall} \tag{2}$$

The radiative heat flux q_r is positive when wall radiates more towards other walls than it is irradiated. It is computed from radiosity J using a high-order method with integration by parts proposed in [2]:

$$q_r = \frac{\epsilon}{1-\epsilon}(\sigma T^4 - J) \tag{3}$$

The wall radiation coupled to natural convection is implemented using the Chebyshev collocation method and validated by Xin *et* al. [7, 2]. For the present Rayleigh-Bénard configurations, the governing N-S equations are discretised on a 61×61 grid for the square cavity and a 121×61 grid for the rectangle cavity. This high-order coupling method allows to use in terms of wall radiation a resolution of 20 points on the vertical wall without affecting the accuracy of results. The use of spectral methods allowed us to check the amplitude of spectral coefficients and ensure that the spatial resolution used is sufficient. In order to calculate unstable solutions and establish bifurcation diagrams, a steady-state solver is also used [7].

3 results

To evidence the influence of wall radiation, simulations are carried out with and without wall radiation in a cavity of aspect ratio AR=1 or 2. Without radiation, the presented results are valid for any cavity height. In presence of wall radiation, the cavity has a height of 3.14cm, a vertical wall emissivity $\epsilon_V = 0.10$ and a horizontal wall emissivity $\epsilon_H = 0.85$ and corresponds to the configuration simulated by Gad & Balaji [1]. In the following, the results are presented in a dimensionless way using the cavity height H as a reference length, ΔT as a reference temperature and $U_{\text{ref}} = \alpha \cdot \text{Ra}^{1/2}/H$ as a reference speed.

3.1 Flow regimes

Bifurcation diagrams established using the x-velocity near the top left cavity corner are presented in Fig. 2 for both cavities. At small Rayleigh numbers without radiation, the well-known stable case is obtained: the fluid is at rest and a stratification of temperature is observed. Wall radiation induces a weak flow near the vertical walls with a 2×2 cell pattern. These solutions at low Rayleigh are denoted S_0. For larger Rayleigh number (up to Ra = 16000 for the square cavity and 8000 for the rectangle cavity), many flow patterns are found like mono-cellular up to 4-cell flows. To make easier the following discussion, flow solutions are named $S_X^{\pm}$ where X is the number of flow-cells and $\pm$ indicates the flow direction at point D (i.e. close to the top left corner).

When Rayleigh number increases gradually in a square cavity, the flow solution S_0 undergoes a perfect supercritical pitchfork bifurcation towards stable mono-cellular flows denoted $S_1^{\pm}$. Solution S_1^+ is ascending along the left wall whereas S_1^- is descending. Wall radiation delays the onset of monocellular flows: a critical Rayleigh number of 2585 is observed without radiation while a value of 2908 is obtained with wall radiation. In the rectangle cavity without radiation, S_0 bifurcates with a perfect pitchfork towards bi-cellular flows at $\text{Ra}_\text{c} = 2013$. With wall radiation, the pitchfork bifurcation becomes imperfect and occurs at a slightly higher value of $\text{Ra}_\text{c} = 2104$. This means that wall radiation keeps the flow symmetry of S_0 (the 2×2 cell pattern observed at lower Rayleigh number) and makes the solution S_0 to bifurcate preferentially towards the ascending solution near the vertical walls (S_2^+) rather than the solution branch S_2^-.

Figure 2 also shows unstable flows obtained by the steady-state solver. In the square cavity without radiation, the unstable solution S_0 bifurcates around Ra = 6743 towards unstable bi-cellular solution $S_2^{\pm}$ with a perfect pitchfork bifurcation. Wall radiation makes again imperfect this pitchfork bifurcation at Ra = 7142. Solutions $S_2^{\pm}$ then become stable after a perfect subcritical pitchfork bifurcation at Ra = 11290 without radiation. In the case with wall radiation S_2 solutions bifurcate respectively at Ra = 11817 and 11844 for the S_2^+ and S_2^- branches. This difference of

Fig. 2a Square cavity, no radiation

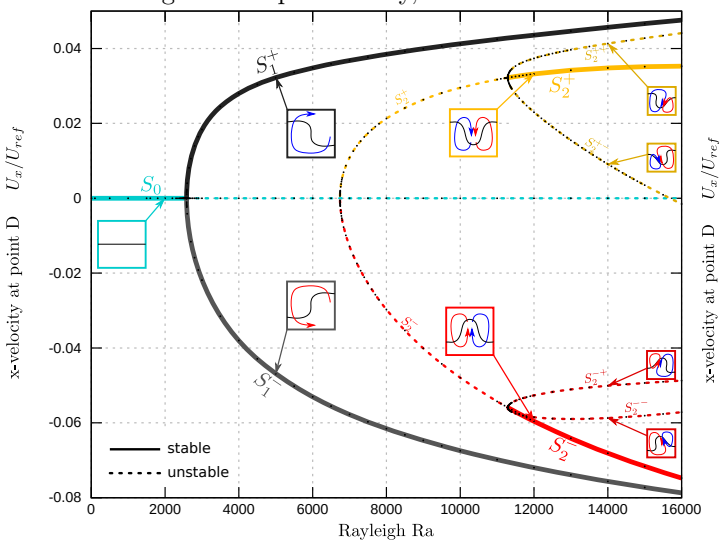

Fig. 2b Rectangle cavity, no radiation

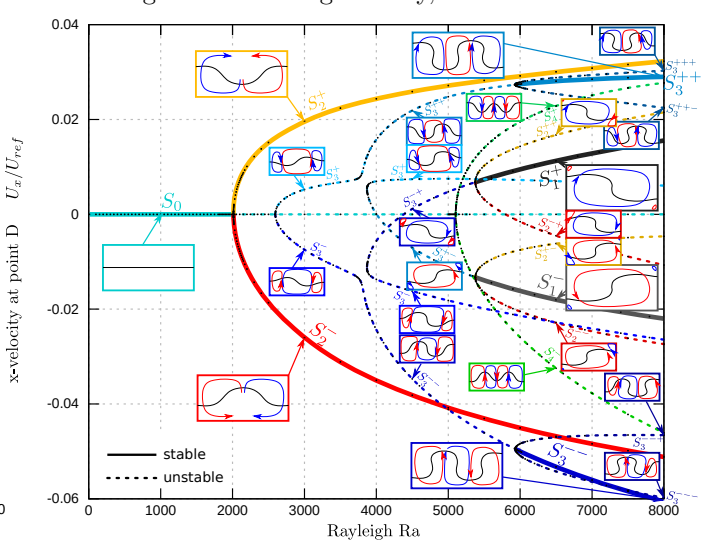

Fig. 2c Square cavity, wall radiation

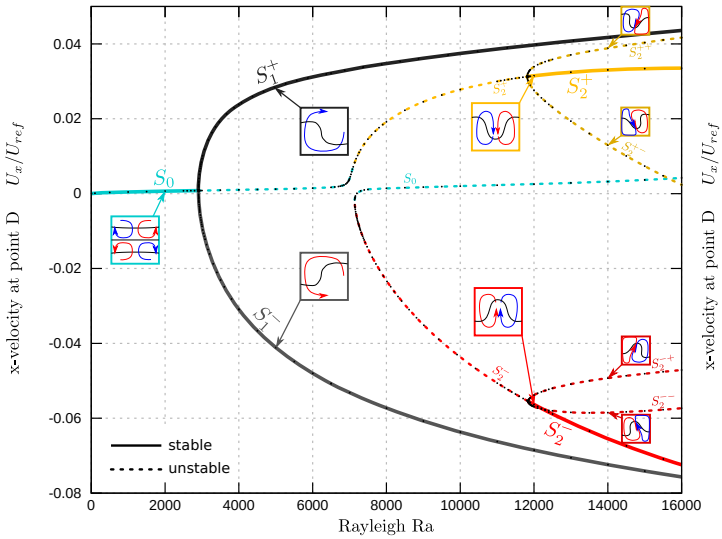

Fig. 2d Rectangle cavity, wall radiation

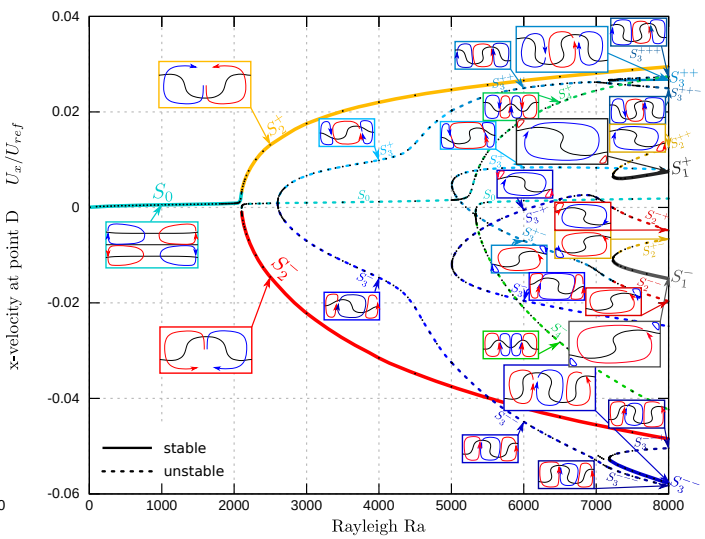

Figure 2: Influence of the aspect ratio and wall radiation illustrated by the bifurcation diagrams using the $x-$velocity at point D in the cavity ($H = 3.14cm$). Some flow patterns are shown (isotherms in black, streamlines in red and blue).

the lower and upper branches comes from the fact that S_2^+ and S_2^- are no longer equivalent after the imperfect bifurcation.

The aspect ratio modifies flow solutions. A greater number of flow patterns is found in the rectangle cavity. Without wall radiation the first bifurcation of S_0 branch is a perfect supercritical pitchfork type and the bifurcated solutions $S_1^{\pm}$ possess two cells. While with wall radiation the first bifurcation of S_0 branch is an imperfect pitchfork type. In both cases, unstable S_0 solutions undergo other bifurcations at higher Rayleigh numbers. At Ra = 16000, flows with one, two or three vertical cells are found in the cavity ($S_1^{\pm}$, $S_2^{\pm}$, S_3^{++} and S_3^{--}).

It is seen that wall radiation keeps almost the same bifurcation diagrams as those observed in the case without radiation and that in the case of wall radiation the bifurcations take place at slightly higher critical Rayleigh numbers. Nevertheless, it should be noted that all the pitchfork bifurcations are perfect and supercritical without radiation and that the pitchfork bifurcations linking S_0-$S_2^{\pm}$, $S_0^{\pm}$-$S_4^{\pm}$, etc. are made imperfect by wall radiation.

3.2 Heat transfer

The heat flux crossing the cavity walls is characterised by radiative and convective Nusselt numbers averaged over the bottom and top walls:

$$\mathrm{Nu_C} = \frac{\overline{q_c}}{k\frac{\Delta T}{H}} \qquad \text{with} \qquad \overline{q_c} = \frac{1}{L}\int_0^L q_c \, dx \tag{4a}$$

$$\mathrm{Nu_R} = \frac{\overline{q_r}}{k\frac{\Delta T}{H}} \qquad \text{with} \qquad \overline{q_r} = \begin{cases} \frac{1}{L}\int_0^L q_r \, dx & \text{at bottom wall} \\ \frac{1}{L}\int_0^L (-q_r) \, dx & \text{at top wall} \end{cases} \tag{4b}$$

The reference heat transfer used for both convection and radiation is pure a conductive flux.

Fig. 3 plots the bifurcation diagrams using the convective Nusselt numbers for both cavities without radiation. Convective Nusselt numbers are the same on the top and bottom walls. The heat transfer rate of one bifurcated branch is the same as the other one.

Fig. 3a Square cavity

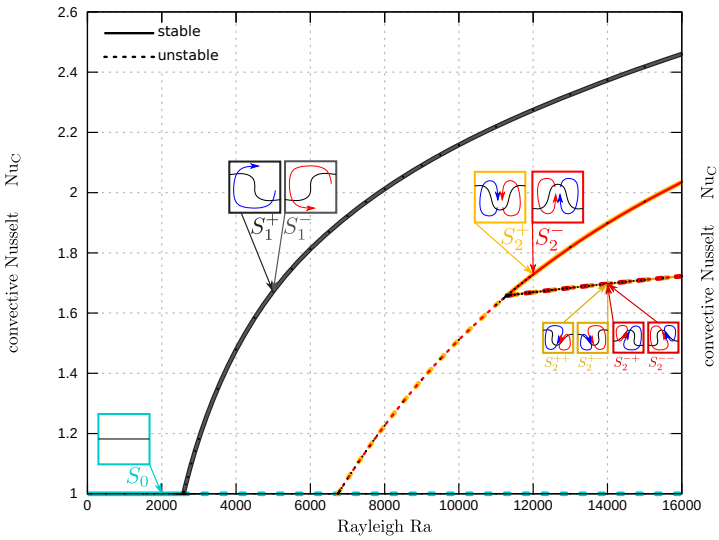

Fig. 3b Rectangle cavity

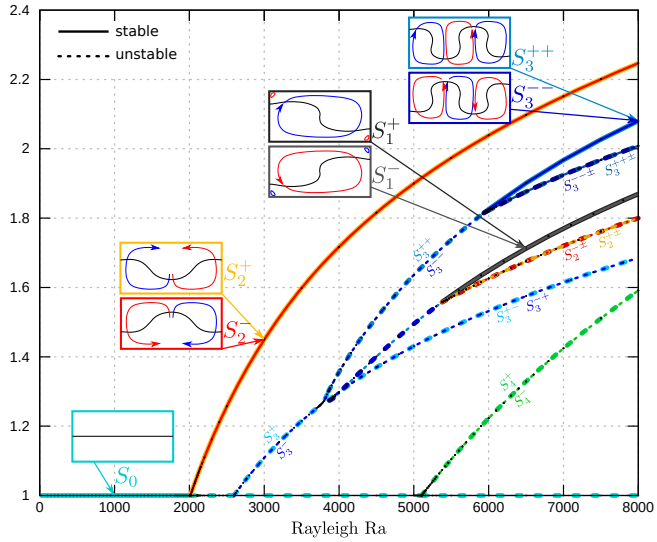

Figure 3: Convective Nusselt number at the bottom wall of a cavity without radiation. Some stable flow patterns are represented.

Fig. 4 shows averaged convective Nusselt numbers in the presence of wall radiation on both the top and bottom walls. It depicts that the bifurcated branches related to any imperfect pitchfork bifurcation (branches $S_2^{\pm}$ and $S_4^{\pm}$ for example) are no longer equivalent and that the averaged convective Nusselt numbers are not the same on the same wall. On the branches bifurcated from a perfect pitchfork bifurcation (branches $S_1^{\pm}$ and $S_3^{\pm}$ for example) convective Nusselt numbers are the same on the same wall. The convective Nusselt numbers on the bottom wall of a square cavity presented in Fig. 4a are in good agreement with the results of [1]. To reach this agreement, the cavity height was set to 3.14cm (i.e. $N_r \simeq 7.765$). The radiation to conduction parameter was not explicitly provided by [1], but it is was deduced from other parameters in the article. Also, it is guessed that their Nusselts are given at the bottom wall because the agreement would be less satisfactory at the top wall.

Radiative Nusselt numbers are represented at the bottom wall in Fig. 5. As stated before, radiative Nusselt numbers on the bifurcated branches related to an imperfect pitchfork birfurcation are different on the same wall. This is the case for $S_2^{\pm}$ and $S_4^{\pm}$, while on those related to a perfect pitchfork birfurcation ($S_1^{\pm}$ and $S_3^{\pm+}$) the same radiative Nusselt is observed.

Values of convective and radiative Nusselt numbers of stable flows at Ra = 2000 and 16000 for the square cavity with wall radiation are given in Table 1. Stable solutions are given at Ra = 2000 or 8000 for the rectangle cavity. The table highlights that convective or radiative Nusselt numbers

Fig. 4a Square cavity: bottom wall

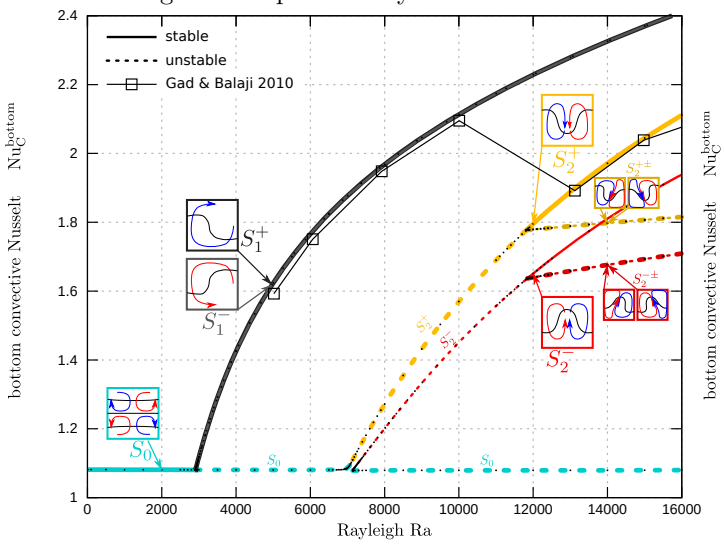

Fig. 4b Rectangle cavity: bottom wall

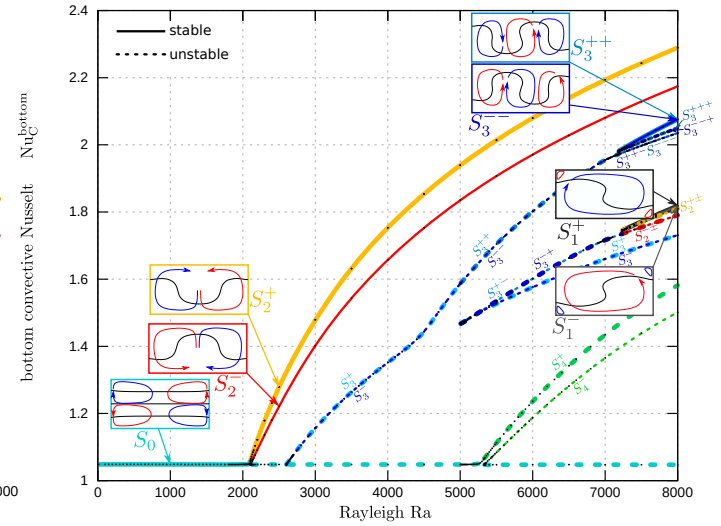

Fig. 4c Square cavity: top wall

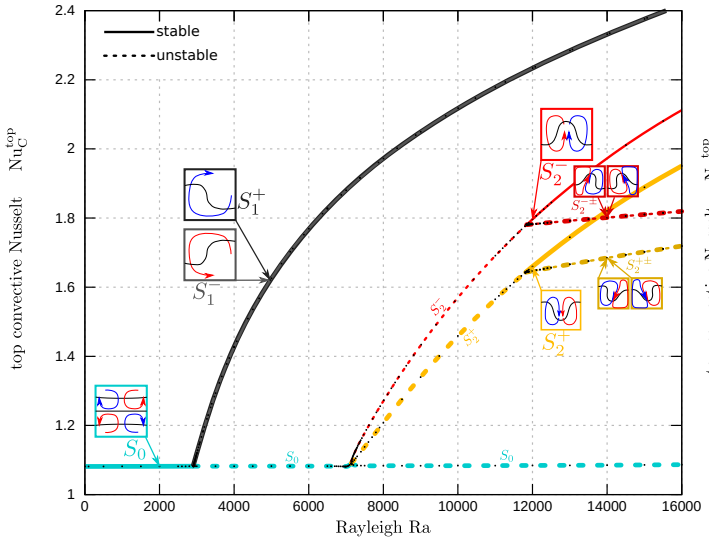

Fig. 4d Rectangle cavity: top wall

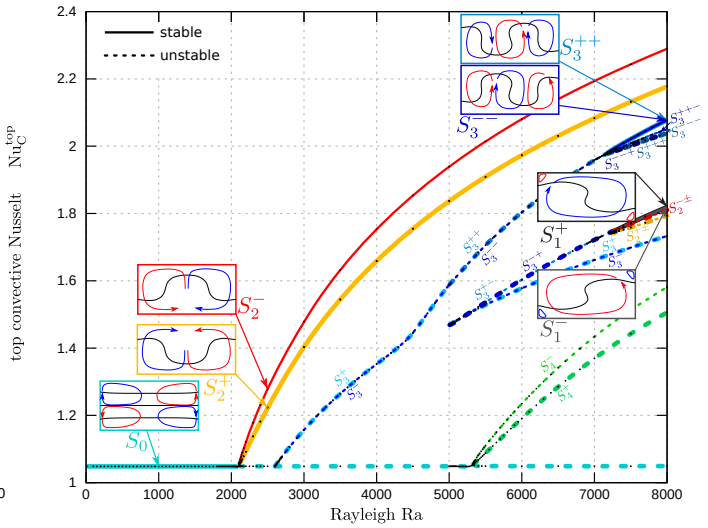

Figure 4: Convective Nusselt numbers on the cavity walls with wall radiation.

are not the same on the bottom wall nor on the top wall in presence of wall radiation. For comparison, convective Nusselt numbers are equal to 1, 2.46 and 2.0346 for respectively S_0, $S_1^{\pm}$ and $S_2^{\pm}$ in the square cavity without radiation. They are equal to 1, 1.8699, 2.2467 and 2.0803 for S_0, $S_1^{\pm}$, $S_2^{\pm}$ and $S_3^{\pm\pm}$ solutions in the rectangle cavity without radiation. These values indicate that wall radiation decreases convective Nusselt numbers except for S_0 and S_2^- solution. The total heat transfer is of course enhanced by wall radiation. It can be checked that the total heat transfer is the same at the top and bottom walls:

$$\mathrm{Nu}_{\mathrm{C}}^{\mathrm{bottom}} + \mathrm{Nu}_{\mathrm{R}}^{\mathrm{bottom}} = \mathrm{Nu}_{\mathrm{C}}^{\mathrm{top}} + \mathrm{Nu}_{\mathrm{R}}^{\mathrm{top}} \tag{5}$$

The sum of convective and radiative Nusselt numbers are null on the left and right walls since they are imposed by the adiabatic condition. Note also that radiative Nusselt numbers are not equivalent for S_2^+ and S_2^- whereas those of S_1^+ and S_3^{++} are equivalent to those of S_1^- and S_3^{--}.

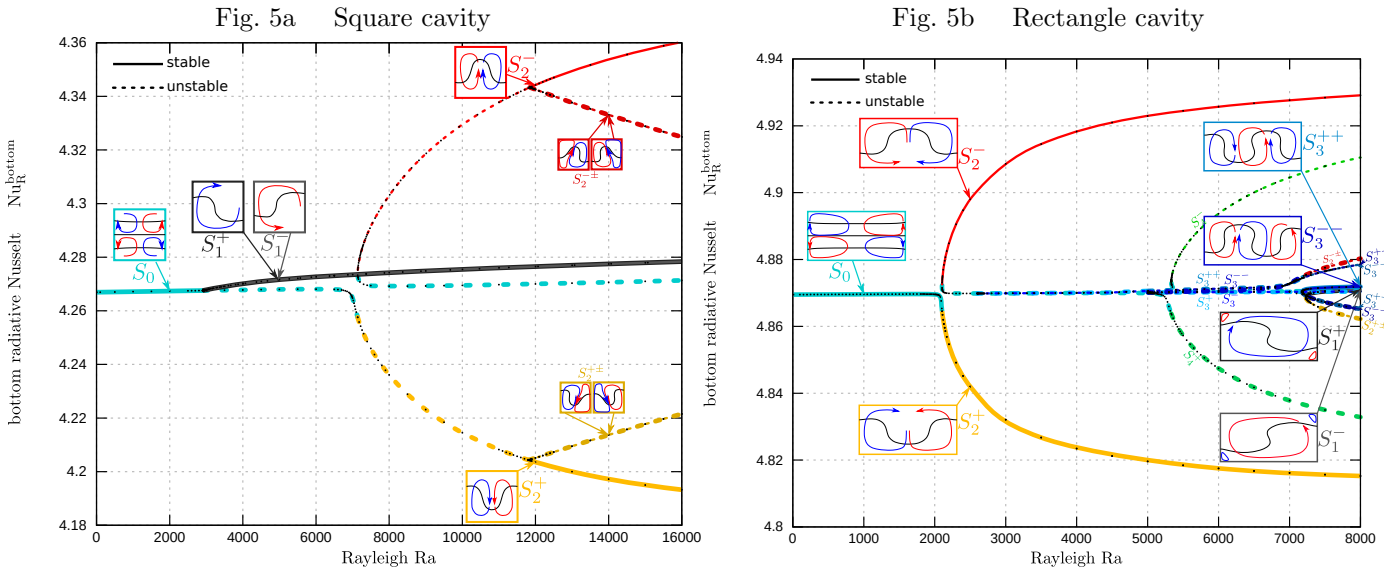

Figure 5: Radiative Nusselt number on the cavity bottom wall.

Table 1: Convective and radiative Nusselt numbers of stable solutions with wall radiation (S_0 solutions are given for Ra = 2000 and other solutions $S_i^{\pm}$ are given at Ra = 16000 for the square cavity and 8000 for the rectangle cavity).

	case	$\mathbf{Nu_C^{left}}$	$\mathbf{Nu_R^{left}}$	$\mathbf{Nu_C^{right}}$	$\mathbf{Nu_R^{right}}$	$\mathbf{Nu_C^{top}}$	$\mathbf{Nu_R^{top}}$	$\mathbf{Nu_C^{bottom}}$	$\mathbf{Nu_R^{bottom}}$
$AR=1$	S_0	$-3.9{\cdot}10^{-4}$	$3.9{\cdot}10^{-4}$	$-3.9{\cdot}10^{-4}$	$3.9{\cdot}10^{-4}$	1.0817	4.2666	1.0810	4.2674
	S_1^+	0.1153	-0.1153	-0.1220	0.1220	2.4176	4.2717	2.4108	4.2784
	S_1^-	-0.1220	0.1220	0.1153	-0.1153	2.4176	4.2717	2.4108	4.2784
	S_2^+	0.0801	-0.0801	0.0801	-0.0801	1.9507	4.3534	2.1109	4.1932
	S_2^-	-0.0868	0.0868	-0.0868	0.0868	2.1128	4.1866	1.9391	4.3603
$AR=2$	S_0	$-1.3{\cdot}10^{-4}$	$1.3{\cdot}10^{-4}$	$-1.3{\cdot}10^{-4}$	$1.3{\cdot}10^{-4}$	1.0484	4.8695	1.0483	4.8696
	S_1^+	0.1194	-0.1194	-0.1214	0.1214	1.8192	4.8699	1.8182	4.8709
	S_1^-	-0.1214	0.1214	0.1194	-0.1194	1.8192	4.8699	1.8182	4.8709
	S_2^+	0.1122	-0.1122	0.1122	-0.1122	2.1771	4.9274	2.2893	4.8152
	S_2^-	-0.1155	0.1155	-0.1155	0.1155	2.2896	4.8136	2.1741	4.9291
	S_3^{++}	0.0971	-0.0971	-0.1002	0.1002	2.0777	4.8703	2.0762	4.8719
	S_3^{--}	-0.1002	0.1002	0.0971	-0.0971	2.0777	4.8703	2.0762	4.8719

4 Conclusions

Simulations have been conducted in a square and a rectangle cavity to investigate the effect of wall radiation on Rayleigh-Bénard convection and heat transfer. Both the cases with wall radiation and without radiation have been investigated and the bifurcation diagrams were established. In both cases many cellular flow branches are encountered at moderate Rayleigh numbers (Ra $\leqslant$ 16000 for the square cavity and Ra $\leqslant$ 8000 for the rectangle cavity). Weak cellular flows are observed even at very low Rayleigh numbers with wall radiation.

It is observed that the bifurcation diagrams are only slightly modified by wall radiation: the corresponding critical Rayleigh numbers increase slightly. Wall radiation makes that convective (and radiative) Nusselt numbers are different on the top and bottom walls. In terms of bifurcation nature, wall radiation introduces a new phenomenon as it makes certain pitchfork bifurcations imperfect. In these cases, the bifurcated branches are no longer equivalent in terms of flow and heat transfer: convective (and radiative) Nusselt numbers are no longer the same on the same

cavity wall.

The present work leads to the following recommendations to describe Bénard convection with wall radiation and more generally natural convection with wall radiation:

- a radiation to conduction parameter (or the cavity height) should always be given since wall radiation depends on the cavity length;
- convective and radiative Nusselt numbers should always be associated to a wall because they are different on the top and bottom walls;
- they should also be associated to a solution branch as the bifurcated branches can be not equivalent.

References

[1] M. A. Gad and C. Balaji. Effect of surface radiation on RBC in cavities heated from below. *International Communications in Heat and Mass Transfer*, 37(10):1459–1464, 2010.

[2] R. Knikker, S. Xin, and R. Dai. High-order numerical implementation of surface radiation for the coupling with natural convection in an air-filled square cavity. In *International Heat Transfer Conference*. IHTC15-9092, Kyoto, Japan, 2014.

[3] A. Langenais, E. Albin, R. Knikker, and S. Xin. Etude numérique de l'influence du rayonnement pariétal sur la convection de rayleigh-bénard en cavité 2d remplie d'air. In *Congrès Français de Thermique*, pages 1–8, 2015.

[4] J. Mizushima and T. Adachi. Sequential transitions of the thermal convection in a square cavity. *Journal of the Physical Society of Japan*, 66(1):79–90, 1997.

[5] E. H. Ridouane, M. Hasnaoui, and A. Campo. Effects of surface radiation on natural convection in a rayleigh-benard square enclosure: steady and unsteady conditions. *Heat and mass transfer*, 42(3):214, 2006.

[6] S. Xin. Méthode de collocation chebyshev pour le couplage entre la convection naturelle en cavité remplie d'air et le rayonnement pariétal. In *20ème Congrès Français de Mécanique, 28 août/2 sept. 2011-25044 Besançon, France (FR)*, pages 1–6. AFM, Maison de la Mécanique, 39/41 rue Louis Blanc, 92400 Courbevoie, France (FR), 2011.

[7] S. Xin, R. Knikker, and R. Dai. Méthodes d'ordré elevé pour le couplage de la convection naturelle avec le rayonnement de surface en cavité remplie d'air. In *Congrès Français de Thermique*, pages 1–8, 2014.